

UC Irvine

UC Irvine Previously Published Works

Title

PREDICTED NASAL AND TRACHEOBRONCHIAL PARTICLE DEPOSITION EFFICIENCIES FOR THE MOUSE

Permalink

<https://escholarship.org/uc/item/7fp6r63f>

Journal

INHALED PARTICLES VII, 38(S1)

Authors

OLDHAM, MJ
PHALEN, RF
SCHUM, GM
[et al.](#)

Publication Date

1994

Copyright Information

This work is made available under the terms of a Creative Commons Attribution License, available at <https://creativecommons.org/licenses/by/4.0/>

Peer reviewed



PREDICTED NASAL AND TRACHEOBRONCHIAL PARTICLE DEPOSITION EFFICIENCIES FOR THE MOUSE*

M. J. OLDHAM, R. F. PHALEN, G. M. SCHUM and D. S. DANIELS

Department of Community and Environmental Medicine, University of California, Irvine,
CA 92717, U.S.A.

Abstract—Few models are available for predicting the efficiency of deposition of inhaled particles in the various regions of the respiratory tract of the mouse. The purpose of this study was to improve the ability to predict upper airway (nose, pharynx and larynx) and tracheobronchial deposition efficiencies for inhaled aerosols in the laboratory mouse. Currently-used equations for predicting nasal deposition efficiencies in humans are semi-empirical and utilize airflow and/or pressure drop data. Therefore, we measured nasal pressure drop and airflow in anaesthetized mice and used this information, together with published data, to formulate aerosol deposition equations. Tracheobronchial deposition efficiency is usually predicted by considering three mechanisms (impaction, sedimentation and diffusion), along with airway anatomical and airflow information. A typical path tracheobronchial airway geometry, complete to the terminal bronchiole, was developed for the mouse from detailed measurements of three replica respiratory tract casts. Particle deposition efficiency calculations were then performed for the tracheobronchial region of the adult mouse and compared with published estimates of aerosol deposition in mice. The calculations, which covered a particle diameter range of 0.1–100 μm (aerodynamic), tended to underestimate the experimental measurements in mice. The calculations did not take into account deposition during exhalation, or the effects of several other complex factors.

INTRODUCTION

BECAUSE the laboratory mouse has been used extensively to study the effects of inhaled substances, the methods of performing inhalation studies are well developed, and a large database on biological effects under a wide variety of conditions exists, it is important to understand the relationship between exposure dose and target tissue dose. However, mathematical equations that use exposure aerosol characteristics in order to predict doses delivered to specific target tissues are not available. Predicted particle deposition efficiency calculations in the mouse have been constrained by the lack of reliable information on upper airways and on the structure of the tracheobronchial tree. We addressed this problem by making upper airway pressure drop vs. airflow measurements and by performing measurements of tracheobronchial airway dimensions for B6C3F₁ mice. The measured resting pressure drop was used with experimental data from RAABE *et al.* (1988) to propose upper respiratory tract deposition efficiency equations. The measured geometry was input into a computer program that used particle deposition equations and airflow rates to obtain calculated particle deposition efficiencies.

Nasal deposition efficiency (N_{eff}) has been predicted for humans by an equation of the form:

*This paper was included in Poster Session 2 and the discussion included in the summary presented in Section 12.

$$N_{\text{eff}} = a + b * \log(D_{\text{ac}}^2 * P), \quad (1)$$

where D_{ac} is the aerodynamic particle diameter and P is the pressure drop across the nose (HOUNAM *et al.*, 1971). In other equations, relationships based on mathematical functions of the airflow are used (STAHLHOFEN *et al.*, 1989). Additionally, a cumulative log-probability fit in the form:

$$N_{\text{eff}} = \frac{1}{1 + e^{-(c + d * (D_{\text{ac}}^2 * P))}} \quad (2)$$

can be used as an alternative to the log-linear equation. The published estimated aerosol deposition efficiencies of RAABE *et al.* (1988) can be used to fit the parameters a , b , c and d if the pressure drop is known. Equations based on pressure drop, unlike those based on airflows, appear to be able to account for variations in body size within a population (HOUNAM *et al.*, 1971).

MATERIALS AND METHODS

The animals used in this study were male B6C3F₁ mice (Harlan Sprague Dawley Inc., Indianapolis, Indiana, U.S.A.). Five mice were used for pressure drop measurements. Twelve lung casts were made and the three most complete were selected for making detailed tracheobronchial tree measurements. The gross characteristics of the animals are shown in Table 1. Pressure drop measurements were made in

TABLE 1. ANIMAL CHARACTERISTICS

	Age (days)	Weight (g)	Length rump to snout (cm)	Chest circumference at axilla (cm)	xyphoid (cm)
Upper airway pressure drop ($N=5$)	78 ± 5.8	25.6 ± 1.0	9.4 ± 0.2	5.7 ± 0.3	6.6 ± 0.4
T.B. cast measurement ($N=3$)	69 ± 1.7	25.8 ± 0.6	9.3 ± 0.3	5.8 ± 0.5	6.8 ± 0.2

All values are stated as mean ± standard deviation.

spontaneously breathing, lightly anaesthetized (by intraperitoneal sodium pentobarbital) mice. A cannula was positioned in the trachea (not pressing against or occluding the larynx) so that the pressure drop measurement included the nose, pharynx and larynx. Air was pulled through the nose into a calibrated glass syringe by a syringe pump (Sage Instruments, Cambridge, Massachusetts, U.S.A.). Pressure was measured relative to the atmosphere by a 'U' tube water manometer.

Tracheobronchial anatomical data were obtained from detailed morphometric measurements of three replica lung casts. The lung casts were made *in situ* using the saline-replacement technique of PHALEN *et al.* (1978). For each of the three silicone rubber (RTV 700, General Electric Corp., Waterford, New York, U.S.A.) casts, the number of generations (trachea = generation 1) to every terminal bronchiole was counted. This was done by examining the casts under a seven-power magnifying lens which allowed terminal bronchioles to be recognized as the last non-alveolarized structure in a pathway. A unique binary identification number was assigned to each airway (PHALEN *et al.*, 1978). In this way, it was possible to track which airways had

been counted and how many generations there were from the trachea to each terminal bronchiole. Correction for any missing airways (which were few, but which were apparent on the casts) was done by counting a substitute pathway with an identical identification number from another cast. Based upon these data, the median number of generations from the trachea to the terminal bronchioles was determined for each cast using a cumulative distribution plot. For each of our casts the median number of generations was 15. In order to obtain a representative 15-generation typical path geometry, we measured and averaged at least 25 pathways from each lung cast. To avoid bias in this selection, every N th 15-generation pathway was selected, where $N=4, 5$ or 7 , depending on the total number of 15-generation pathways in the cast. Table 2 shows the lung cast characteristics, including measurement sampling strategy

TABLE 2. MOUSE LUNG CAST CHARACTERISTICS

Cast number	Range of generations in TB	Median generation	Number of median generation paths	Median generation sampling strategy	Total paths
1	6-27	15	125	Every fifth path	25
2	6-27	15	119	Every fourth path	30
3	6-26	15	175	Every seventh path	25

and the total number of measured paths in each lung cast. Every airway in the path was measured for airway length, diameter and branch angle. Inclination to gravity was measured on selected airways. Measurements were averaged by generation for each animal. The average values for the individual animals were then averaged together to establish a typical path tracheobronchial geometry.

To calculate tracheobronchial particle deposition efficiencies, the particle deposition equations of YEH and SCHUM (1980) were used, along with minute ventilation values, 25 and 50 ml (equivalent to steady inspiratory airflow rates of 50 and 100 ml min^{-1}), from the equation of GUYTON (1947) and airway geometry determined in this study. Two ventilation rates were used in order to cover the physical activity range of resting to a moderate level of exercise.

RESULTS

Despite the close matching (with respect to age, body length and weight) of the mice used in the upper airway pressure vs airflow measurements, individual variation was large. Therefore, these measurements were only used to select a pressure drop that was believed to be representative of that during resting ventilation. This value was needed for converting the deposition data of RAABE *et al.* (1988) into empirical relationships. Our inspiratory nasal airflow vs pressure drop data indicated that for a likely 27 ml resting minute ventilation of the RAABE *et al.* (1988) animals, the upper respiratory tract pressure drop was about 93.5 mm H_2O . RAABE *et al.* (1988) obtained particle deposition data from analysing tissues obtained after particle deposition; therefore, we corrected the data for particle clearance. The correction for particle clearance was performed by apportioning the radiolabel found in the GI tract to the upper airway and to the tracheobronchial regions. The ratio of sacrifice-time label contents in these

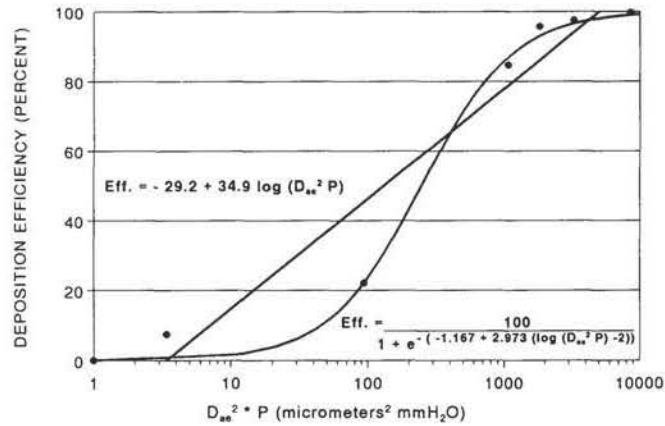


FIG. 1. Upper airway particle deposition in the B6C3F₁ mouse as a function of particle size and pressure drop. Efficiencies from measurements by RAABE *et al.* (1988) of head deposition efficiency of radioactive monodisperse particles in CF₁ mice (the measurements were corrected to include some material cleared to the G.I. tract) are also shown.

regions was used to distribute the amount reported in the GI tract. Both log-linear and cumulative log-probability regressions were used to express deposition efficiency as a function of $\log(D_{ac}^2 \times P)$, as shown in Fig. 1. The units for $D_{ac}^2 \times P$ in the equations are $\mu\text{m}^2 \text{mm H}_2\text{O}$. We were unable to establish a clear relationship between upper airway pressure drop and airflow. In humans the two are related through a simple power function. In mice, as in rats (KIMBALL and MORGAN, 1991), it is possible that active nostril musculature allows those animals to maintain a relatively low pressure drop at high airflow rates. Figure 1 indicates that a log-linear fit of the same type used for humans by HOUNAM *et al.* (1971) has an $r^2=0.42$ (r^2 =ratio of regression sum of squares to total sum of squares) and the cumulative log-probability fit has a pseudo $r^2=0.99$ (pseudo $r^2=1$ —ratio of weighted residual sum of squares to $N-1$ times the weighted variance).

The typical-path mouse tracheobronchial geometry is shown in Table 3. Predicted tracheobronchial deposition efficiencies (Fig. 2) for steady inspiratory flows for the adult mouse at 50 and 100 ml min^{-1} were calculated for particles with aerodynamic diameters from 0.1 to 100 μm using the YEH and SCHUM (1980) equations. Also shown in the figure are the experimental data of RAABE *et al.* (1988), normalized to the amount entering the trachea, and again with some clearance taken into account through a simple correction.

DISCUSSION

As shown in Fig. 1, the cumulative log-probability fit of the RAABE *et al.* (1988) data is superior to the log-linear fit. The cumulative log-probability fit also does not predict deposition efficiencies less than 0% or greater than 100%. Both semi-empirical equations represent fits to data corrected for mucociliary clearance. For simplicity, it was assumed that mucociliary clearance rates were equivalent in the upper respiratory

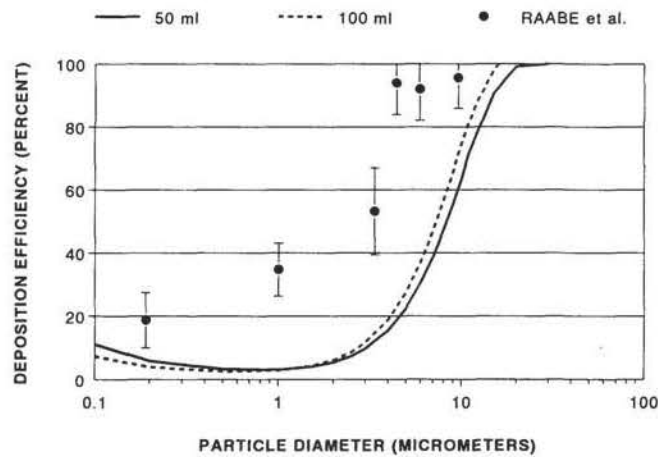


FIG. 2. Predicted inspiratory particle deposition efficiencies in the tracheobronchial tree of an adult mouse using steady inspiratory flows of 50 and 100 ml min⁻¹. The experimental data of RAABE *et al.* (1988) (the measurements were corrected to include some of the G.I. tract radioactivity and normalized to material entering the trachea) are also shown. The aerodynamic equivalent diameter is presented. This diameter is calculated from the original reported aerodynamic resistance diameter using the method of RAABE (1976).

TABLE 3. UCI TYPICAL PATH TRACHEOBRONCHIAL GEOMETRY FOR THE B6C3F₁ MOUSE (MEANS AND SE)

Generation number	Airway length (mm)		Airway diameter (mm)		Branch angle (°)		Gravity angle (°)		Number of airways
	\bar{X}	SE	\bar{X}	SE	\bar{X}	SE	\bar{X}	SE	
1	8.97	0.18	1.37	0.05	0	0	90	0	1
2	5.08	0.15	1.41	0.10	14	1	78	3	2
3	2.02	0.08	1.14	0.11	18	2	85	7	4
4	0.83	0.12	0.90	0.09	30	4	77	3	8
5	0.97	0.15	0.78	0.08	12	2	71	6	16
6	0.50	0.02	0.72	0.03	10	2	71	4	32
7	0.43	0.04	0.63	0.03	11	3	60	N/A	50
8	0.43	0.01	0.54	0.02	10	0	60	N/A	75
9	0.40	0.02	0.45	0.01	16	2	60	N/A	115
10	0.34	0.02	0.40	0.00	11	3	60	N/A	175
11	0.33	0.01	0.36	0.01	12	1	60	N/A	270
12	0.27	0.01	0.29	0.01	18	3	60	N/A	420
13	0.24	0.01	0.21	0.01	22	3	60	N/A	640
14	0.18	0.01	0.14	0.01	33	6	60	N/A	980
15	0.13	0.00	0.10	0.00	61	1	60	N/A	1505

Note: gravity angle for trachea was assumed to be 90°. Generations 2–6 used the trachea as a reference and generations 7–15 were assigned a gravity angle of 60° as unbiased direct measurements were not possible.

tract and the tracheobronchial region. It should also be noted that two resting minute ventilations were used—27 ml for the upper respiratory tract, and 25 ml for the tracheobronchial region. This was due to the average difference in weight (5 g) between the animals used by RAABE *et al.* (1988) and the animals used in our study. When the

respective weights are used in GUYTON's (1947) equation, slightly different minute ventilations result.

Other typical path lung geometries have been based on as few as one replica cast (WEIBEL, 1963; YEH and SCHUM, 1980) or as many as 20 replica casts (PHALEN *et al.*, 1985). The mouse typical path lung geometry is based upon three replica lung casts. A measure of anatomical variation from closely matched animals can be obtained from Table 3, where each value is an average of three animals. The standard error of airway lengths and diameters ranged from 0 to 15% of the airway length, and from 0 to 10% of the airway diameter. The average standard error was 5.5% for airway length and 4.9% for airway diameter. PHALEN *et al.* (1990) showed that for a given anatomy and given particle size, variation in airway lengths and diameters of 5% typically resulted in expected differences in predicted deposition efficiencies of less than 10%.

Comparison of our predicted aerosol deposition efficiencies in the tracheobronchial tree with the experimental data of RAABE *et al.* (1988) in Fig. 2 show that the predicted efficiencies are significantly lower. Several factors may influence this comparison. The actual ventilation rate of the animals in the RAABE *et al.* (1988) experiment were not measured, but it was assumed to be a resting ventilation. Ventilation in exposure setups can presumably vary from that of sleeping animals to that of high activity if the animals are trying to escape. More accurate mathematical predictions are dependent upon accurate ventilation data obtained during the exposure. The mathematical predictions also do not account for the effects of the larynx on deposition in the trachea and bronchial regions, cyclical airflow during breathing, deposition during exhalation, or particle clearance effects in the pulmonary or tracheobronchial region. Therefore, our curves for predicting the deposition of aerosols inhaled by mice must, be considered as rudimentary.

Acknowledgements—This research was supported by the Nickel Producers Environmental Research Association. Support for the computer modelling was provided by the National Heart, Lung and Blood Institute (ROI HL 39682). The authors wish to thank Ms Marie Tonini and Ms Sonia Usdansky for manuscript preparation.

REFERENCES

- GUYTON, A. C. (1947) Measurement of the respiratory volume of laboratory animals. *Am. J. Physiol.* **150**, 70–77.
- HOUNAM, R. E., BLACK, A. and WALSH, M. (1971) The deposition of aerosol particles in the nasopharyngeal region of the human respiratory tract. *J. Aerosol Sci.* **2**, 47–61.
- KIMBELL, J. S. and MORGAN, K. T. (1991) Airflow effects on regional disposition of particles and gases in the upper respiratory tract. *Radiat. Protect. Dosim.* **38**, 213–219.
- PHALEN, R. F., OLDHAM, M. J., BEAUCAGE, C. B., CROCKER, T. T. and MORTENSEN, J. D. (1985) Postnatal enlargement of human tracheobronchial airways and implications for particle deposition. *Analyt. Rec.* **212**, 368–380.
- PHALEN, R. E., SCHUM, G. M. and OLDHAM, M. J. (1990) The sensitivity of an inhaled aerosol tracheobronchial deposition model to input parameters. *J. Aerosol Med.* **3**, 271–282.
- PHALEN, R. F., YEH, H. C., SCHUM, G. M. and RAABE, O. G. (1978) Application of an idealized model to morphometry of the mammalian tracheobronchial tree. *Analyt. Rec.* **190**, 167–176.
- RAABE, O. G. (1976) Aerosol aerodynamic size conventions for inertial sampler calibration. *J. Air Pollut. Contr. Ass.* **26**, 856–860.
- RAABE, O. G., AL-BAYATI, M. A., TEAGUE, S. V. and RASOLT, A. (1988) Regional deposition of inhaled monodisperse coarse and fine aerosol particles in small laboratory animals. In *Inhaled Particles VI*

- (Edited by DODGSON, J., MCCALLUM, R. I., BAILEY, M. R. and FISHER, D. R.), pp. 53–63. Pergamon Press, Oxford.
- STAHLHOFEN, W., RUDOLF, G. and JAMES, A.C. (1989) Intercomparison of experimental regional aerosol deposition data. *J. Aerosol Med.* **2**, 285–308.
- WEIBEL, E. R. (1963). *Morphometry of the Human Lung*. Springer, Berlin.
- YEH, H. C. and SCHUM, G. M. (1980) Models of human lung airways and their application to inhaled particle deposition. *Bull. Math. Biol.* **42**, 461–480.